RAPID COMMUNICATIONS

PHYSICAL REVIEW B VOLUME 50, NUMBER 11 15 SEPTEMBER 1994-I

Structural analyses of ordered rubidium phases on Ru(0001) using low-energy electron diffraction

T. Hertel, H. Over, H. Bludau, M. Gierer, and G. Ertl

Fritz-Haber-Institut der Max-Planck-Gesellschaft, Faradayweg 4-6, D-14195 Berlin (Dahlem), Federal Republic of Germany

(Received 23 May 1994; revised manuscript received 13 July 1994)

The adsorption geometries of the $p(2\times2)$ and $(\sqrt{3}\times\sqrt{3})R30°$ Rb/Ru(0001) phases at coverages of 0.25 and 0.33, respectively, were investigated using low-energy electron diffraction. The structure analyses revealed that Rb resides in the threefold fcc site in the $p(2\times2)$ phase while for the $(\sqrt{3}\times\sqrt{3})R30°$ phase the hcp site is favored. The effective radius of Rb does not change with the Rb coverage within the error bars of this analysis. The concept of "split positions" has been used in order to take the enhanced motion of the adsorbate atoms parallel to the surface properly into account.

The adsorption of alkali metals on metal surfaces has attracted growing attention in the past five years, during which the interpretation of experimental results and theoretical findings led to controversial (and somewhat semantic) discussions about the corresponding bonding character. Simple classifications like covalent or ionic bonding were used to describe the complex adsorption mechanism of alkali metals (AM's) on metals surfaces, triggering off this controversy. In the past, the widespread interest has been based on the key role alkali metals play in heterogeneous catalysis[1] and their role as a seemingly simple model system for studying the chemisorption process in detail. At present, the interest has been spurred by many unexpected findings concerning the adsorption geometries and also by *ab initio* calculations showing a new quality of agreement with experimental findings.[2–10]

The alkali-metal–Al(111) system, e.g., has been studied extensively. Surface-extended x-ray-absorption fine structure measurements performed by Haase and co-workers[2] came up with a very unusual adsorption site, namely, the quasisubstitution of Al-substrate atoms by Na atoms. Subsequent theoretical investigations corroborated this result on the basis of total-energy calculations.[2,3] For the adsorption of K, Na, and Rb on the Al(111) surface at low temperatures, it was shown that the metastable on-top adsorption site transforms irreversibly into the substitutional adsorption configuration upon warming up the sample.[4,6,7] For a survey of experimental and theoretical findings on these systems the reader might be referred to Andersen *et al.*[7]

Another interesting system represents AM adsorption on Ru(0001). The Cs-, K-, and Na-Ru(0001) systems[8–10] have shown coverage-dependent adsorption sites for the $p(2\times2)$ and the $(\sqrt{3}\times\sqrt{3})R30°$ phases at coverages of $\frac{1}{4}$ and $\frac{1}{3}$, respectively. At a coverage of $\frac{1}{3}$, the threefold hcp site was preferred in all these systems. In the $p(2\times2)$ phases, on the other hand, Cs occupies the on-top site while for potassium and sodium overlayers the threefold fcc site was determined. Thus, the "traditional view" that (metal) adsorbates on a metal substrate should occupy those adsites, which continue the stacking sequence of the substrate crystal,[11] was only confirmed with the high-coverage $(\sqrt{3}\times\sqrt{3})R30°$ phases. It has been argued that the observed hcp-site occupation is correlated with the fact that at a coverage of $\frac{1}{3}$ the electronic character of these adlayers is essentially metallic.[9,10] The observation of "unexpected" adsites like the on-top or fcc site in the low-coverage phases was therefore attributed to a shift in the delicate energy balance due to the complex interplay of adsorbate-adsorbate (A-A), adsorbate-substrate (A-S), and substrate-mediated interactions (e.g., screening). Physical quantities that are of particular interest in this context are the dipole moment, which governs the (A-A) interaction, and the size of the AM atoms, which strongly influence the net corrugation potential, as it is experienced by the adsorbate particles.

The different adsites found for the Ru(0001)-$p(2\times2)$-Cs phase (top) and the Ru(0001)-$p(2\times2)$-K phase (fcc) drew our attention to rubidium, which is the missing link between Cs and K among the AM's. Not only the position in the Periodic Table but also the size and the initial-dipole moment of adsorbed Rb provide a connection between K and Cs. Would Rb occupy the on-top or the fcc position or even another site? In answering this question, we report on low-energy electron-diffraction (LEED) structure analyses of the $p(2\times2)$ and the $(\sqrt{3}\times\sqrt{3})R30°$ phases of the Rb/Ru(0001) system at coverages of $\frac{1}{4}$ and $\frac{1}{3}$, respectively. We found that for the low-coverage $p(2\times2)$ phases Rb atoms reside in the threefold fcc sites, while in the $(\sqrt{3}\times\sqrt{3})R30°$ phase the hcp site is again favored. Hence, the observation of on-top site adsorption on Ru(0001) is restricted to the case of cesium.

The experiments were performed in a UHV chamber at a base pressure of 6×10^{-11} mbar. Details about the experimental setup and sample preparation can be found elsewhere.[8] Rubidium was evaporated from a well-outgassed dispenser source (SAES Getters, Inc.). I-V curves were measured at normal incidence and a sample temperature of 50 K using a four-grid display LEED optics. A computer-controlled video LEED system was used to record integrated spot intensities from the fluorescent screen. The desired Rb coverages were achieved by flashing the sample to certain temperatures after deposition of a multilayer Rb film. The optimum coverages were judged from the quality of the $(\sqrt{3}\times\sqrt{3})R30°$ and the (2×2) LEED pattern, and finally cross-checked by the integral of corresponding Rb thermal desorption spectra.

0163-1829/94/50(11)/8126(4)/$06.00

Nine spin-averaged phase shifts were used for the computation of the I-V curves. Details about their computation can be found in Ref. 8. The discrepancy between experimental and theoretical intensity data was quantified both by using the r_{DE} factor introduced by Kleinle *et al.*[12] and by Pendry's r factor r_P.[13] For the Ru layers the phase shifts were temperature corrected using a fixed effective Debye temperature of 420 K. In order to account for the effect of anisotropic adsorbate vibrations on the beam intensities, we invoked the concept of "split positions," which has been introduced in low-energy electron diffraction and successfully applied to the Ru(0001)-$(\sqrt{3}\times\sqrt{3})R30°$-CO system.[14] It has been found that the carbon monoxide molecule, which is adsorbed in the on-top position, revealed a bending-mode vibration with a large amplitude that is compatible with corresponding electron-stimulated-desorption ion angular distribution results.[15]

For the alkali-metal–Ru(0001) system, the vibrational motions of AM atoms are expected to be comparably anisotropic, i.e., thermally induced vibrations of the adparticle parallel to the surface should be much softer than perpendicular ones. This may be explained by the small corrugation potential imposed by the Ru(0001) surface; note that the bigger the AM atom the less corrugated is this potential.[3] Inelastic He scattering at AM adsorbed on graphite, e.g., revealed phonon modes with excitation energies of 2–7 meV,[16] which correspond to large mean-square displacements away from the equilibrium position. This would certainly also have an influence on measured LEED intensities. In fact, it has been speculated that strong anisotropic motions of AM atoms give rise to the commonly observed poor r factors for these systems.[17] This clearly calls for a method that is able to model anisotropic-temperature effects within the multiple-scattering formalism. Very recently such a method has been supplied, the so-called "split-positions,"[14] which will briefly be discussed in the following. If we assume a parametric dependence of the amplitude $A_{\mathbf{g}}$ of individual beams on the displacement of Rb $\Delta\mathbf{r}$ away from its equilibrium position, we may write for the measured intensity $I_{\mathbf{g}}$ of a certain beam,

$$I_{\mathbf{g}}=\langle A_{\mathbf{g}}\rangle_T^2, \quad \langle A_{\mathbf{g}}\rangle_T=\int A_{\mathbf{g}}(\Delta\mathbf{r})\rho(\Delta\mathbf{r},T)d^3\Delta\mathbf{r}, \tag{1}$$

where T is the substrate temperature, ρ is the distribution function, and $\mathbf{g}$ is the reciprocal-lattice vector characterizing a specific LEED beam. Here, the measured intensity is interpreted as a coherent summation over scattering contributions from a statistical ensemble of atoms displaced by $\Delta\mathbf{r}$ from their equilibrium positions. In the case of isotropic parallel motion of Rb with both lateral and vertical vibrations being harmonic and decoupled, the probability density distribution $\rho(\Delta\mathbf{r},T)$ is simply given by the product $\Delta r_{\parallel}\rho_G(\Delta r_{\perp};\omega_{\perp};T)\rho_G(\Delta r_{\parallel};\omega_{\parallel};T)$ of Gaussian distribution functions. The only free parameters are the excitation energies of these vibrations, $\hbar\omega_{\parallel}$ and $\hbar\omega_{\perp}$. Utilizing polar coordinates, the amplitude in Eq. (1) takes on the following form:

$$\langle A_{\mathbf{g}}\rangle_T=\int\int\left[\int A_{\mathbf{g}}(\Delta r_{\parallel};\varphi;\Delta r_{\perp})d\varphi\right]\rho_G(\Delta r_{\parallel};\omega_{\parallel};T)\times\Delta r_{\parallel}\rho_G(\Delta r_{\perp};\omega_{\perp};T)d\Delta r_{\parallel}d\Delta r_{\perp}. \tag{2}$$

The Gaussian distribution functions are given by

$$\rho_G(\Delta r_{\parallel};\omega_{\parallel};T)=\frac{1}{\pi\langle\Delta r_{\parallel}^2\rangle_T}e^{-\Delta r_{\parallel}^2/\langle\Delta r_{\parallel}^2\rangle_T},$$
$$\rho_G(\Delta r_{\perp};\omega_{\perp};T)=\left(\frac{1}{2\pi\langle\Delta r_{\perp}^2\rangle_T}\right)^{1/2}e^{-\Delta r_{\perp}^2/2\langle\Delta r_{\perp}^2\rangle_T}, \tag{3}$$

with the mean-square displacements

$$\langle\Delta r_{\parallel}^2\rangle_T=\frac{\hbar}{m\omega_{\parallel}}\coth\left[\frac{\hbar\omega_{\parallel}}{kT}\right],$$
$$\langle\Delta r_{\perp}^2\rangle_T=\frac{\hbar}{2m\omega_{\perp}}\coth\left[\frac{\hbar\omega_{\perp}}{kT}\right]. \tag{4}$$

The averaging over scattering contributions from atoms at different azimuthal angles φ is performed in the integral over φ and simulated by split positions.[14] Each of these positions is occupied with equal weight, and the calculations are performed within the framework of the averaged T-matrix approximation method,[18] suppressing all multiple-scattering paths between the split positions belonging to one adsite. The integral over the radial component $\Delta r_{\parallel}$ averages over contributions from different displacements $\Delta r_{\parallel}$. This integral can be well approximated by using two or three distinct displacements $\Delta r_{\parallel}$ away from the equilibrium position. The integral over $\Delta r_{\perp}$ was modeled by two to three perpendicular displacements. If the Gaussian distribution function for lateral motion is narrow, i.e., for higher excitation energies, the corresponding distribution can even be well approximated by a single value $\Delta r_{\parallel}$, which in this case represents the mean-square deviation of that vibration. A more detailed account of the concept of split positions will be given elsewhere.[19]

Besides the structural parameters, the vibration frequencies $\omega_{\parallel}$ and $\omega_{\perp}$ describing the harmonic motion parallel and perpendicular to the surface are also refined during the optimization run. Recall that these frequencies characterize the distribution function in the harmonic approximation.

For the structural analysis of the $p(2\times2)$ structure, a total number of 411 data points corresponding to a total energy range of 2055 eV in three integer and six fractional order beams were used for comparison with experiment. In the first grid search we varied the Rb-Ru and first Ru interlayer spacings for Rb adsorbed on either of the four high-symmetry adsorption sites, namely, the fcc, hcp, on-top, or bridge site. Here, the r factors already indicated a clear preference for the threefold fcc site. In the next step the four optimum geometries served as starting configurations in a nonlinear least-squares optimization scheme—with respect to intensities or the Y functions—allowing simultaneous refinement of structural parameters and the real part of the muffin-tin zero.[20–22] The optimization was performed with and without the use of split positions. The preference for the fcc site was not affected by the optimization scheme, and it could be enhanced even further when split positions were included. Best-fit r factors for the individual geometries, with and without applying the concept of split positions, are collected in Table I. For the fcc geometry the r_{DE} factor improved by 0.05 while Pendry's r factor r_P improved by even 0.11 when a distribution of lateral split positions equivalent to an exci-

TABLE I. Optimum r factors for different adsorption sites of the Rb in the (2×2) structure neglecting and/or considering anisotropic motions of Rb.

Adsite	Split position	r_{DE}	r (Pendry)
on top	no	0.59	0.69
	yes	0.52	0.65
bridge	no	0.48	0.58
	yes	0.44	0.52
fcc	no	0.43	0.45
	yes	0.38	0.34
hcp	no	0.47	0.60
	yes	0.44	0.52

tation energy of $h\omega_{\parallel}=2.0\pm0.5$ meV (this corresponds to a mean-square deviation of about 0.37 Å) and a vertical vibration of 10 ± 4 meV were introduced. The final level of agreement between theoretical and experimental I-V curves can be seen from Fig. 1. Structural parameters of the best fit geometry of Rb-(2×2) are depicted in Fig. 2.

The same procedure has been applied to obtain structural data for the Rb-$(\sqrt{3}\times\sqrt{3})R30°$ phase using a total number of 316 data points corresponding to a total energy range of 1580 eV in three integer and five fractional order beams. As with Na, K, and Cs adsorbed on Ru(0001), the occupation of the hcp site is clearly favored, as seen from Table II. Also for this phase, the introduction of split positions was able to significantly decrease the r factors: The corresponding excitation energies for lateral and vertical vibrations were the same as those found with the Rb-(2×2) structure within the uncertainties. Structural parameters for the Rb-$(\sqrt{3}\times\sqrt{3})R30°$ phase are summarized in Fig. 3. The comparison of theoretical and experimental I-V data for the optimum structure is shown in Fig. 4.

The results from the structural analysis of the Cs/Ru(0001) system[23] and the K/Al(111) system,[24] applying the concept of split positions, indicates that the agreement between experimental and calculated I-V data is also substantially improved; for Cs/Ru(0001)-(2×2), the in-plane motion of Cs turned out to be even larger, namely, about 0.5 Å, corresponding to an excitation energy of 1.5 ± 0.5 meV.

The reductions in the r factors, when employing the concept of split positions, suggest that frequently more reliable

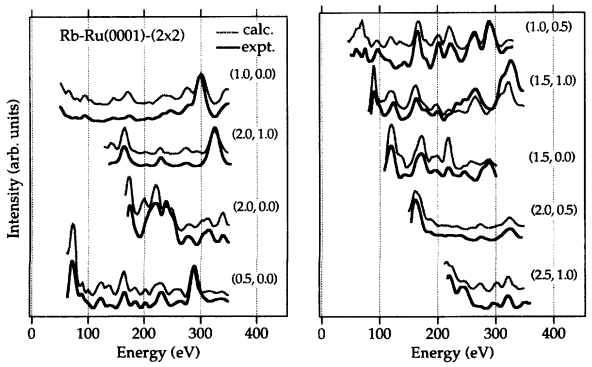

FIG. 1. Comparison of the experimental and calculated best-fit I-V curves for the Ru(0001)-(2×2)-Rb system ($r_{DE}=0.38$, $r_P=0.34$). Adsorption site of Rb, fcc site.

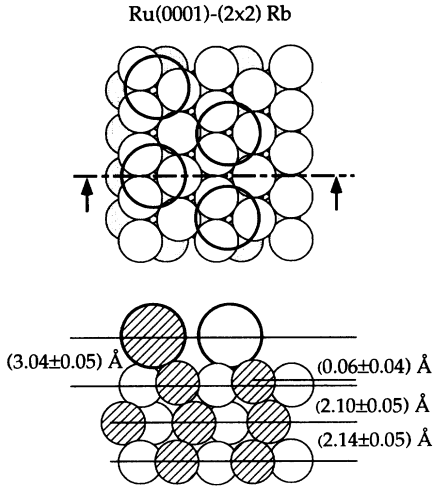

FIG. 2. Top view and side view of the optimum structure model for the Ru(0001)-(2×2)-Rb phase. Structural parameters are indicated. Large circles, Rb; smaller circles, Ru. Lateral distortions of Ru atoms in the top layer have not been found.

LEED-structure analyses have been hampered in the past partly by the presence of strong anisotropic atomic motions. Considering the improvement of the reliability of structural analyses, this treatment appears to be more promising than an attempt made by Fritzsche *et al.*[25] There the authors tried to account for the modification of the scattering potential, which is introduced by the AM-induced dipole layer at the surface. In fact, this led to a slightly better agreement of the fractional-order beams; however, the averaged r factor did not change. As seen from Table I, the averaged r factors in our LEED analyses decreased by 0.11 and 0.07 for the Rb/Ru(0001)-(2×2) and $(\sqrt{3}\times\sqrt{3})R30°$ phases, respectively.

An interpretation of the found lateral mean-square deviation of about 0.37 Å is not straightforward, because the LEED analysis cannot discriminate between static and dynamic disorder as long as only I-V curves for a single sample temperature are considered. To resolve this problem, temperature-dependent measurements are needed. However, from a comparison of this result with results found by He scattering on the AM-graphite system, it seems to be reasonable to discuss the found split positions in terms of a lateral vibrational mode of Rb. The corresponding excitation energy of roughly 2.0 ± 0.5 meV for the lateral vibration of Rb (in

TABLE II. Optimum r factors for different adsorption sites of the Rb in the $(\sqrt{3}\times\sqrt{3})R30°$ structure neglecting and/or considering anisotropic motions of Rb.

Adsite	Split position	r_{DE}	r (Pendry)
on top	no	0.66	0.60
	yes	0.64	0.60
bridge	no	0.41	0.57
	yes	0.40	0.57
fcc	no	0.50	0.65
	yes	0.44	0.61
hcp	no	0.47	0.35
	yes	0.38	0.28

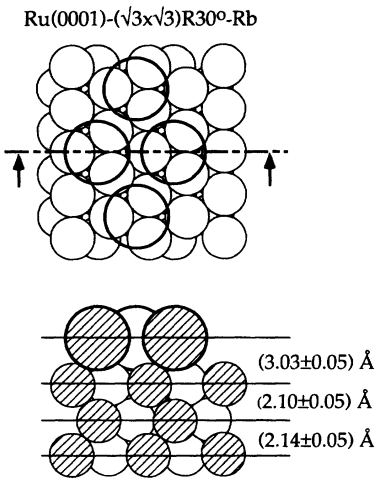

FIG. 3. Top view and side view of the structural model and parameters for the best-fit arrangement of the Ru(0001)-$(\sqrt{3}\times\sqrt{3})R30°$-Rb phase. Large circle, Rb; smaller circles, Ru. Lateral distortions of Ru atoms in the top layer have not been observed.

the Einstein model) is in remarkably nice agreement with values found with the Rb-graphite system (2.8 meV).[16]

The structural results indicate that Rb behaves similarly to potassium rather than to cesium. Again, for both coverages of Rb the occupation of threefold-hollow sites has been found, and the effective Rb radius of 2.07 Å does not change

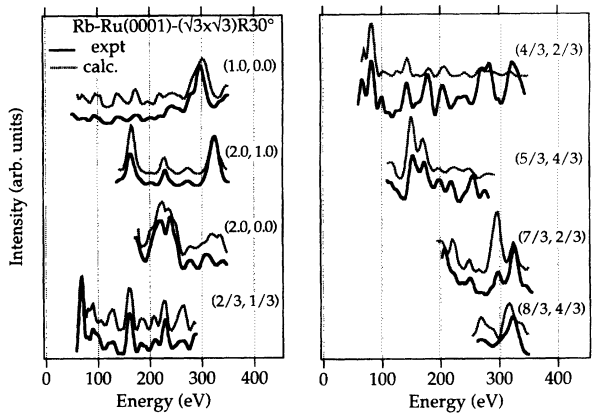

FIG. 4. Comparison of the experimental and calculated best-fit *I-V* curves for the Ru(0001)-$(\sqrt{3}\times\sqrt{3})R30°$-Rb system ($r_{DE}=0.38$, $r_P=0.34$). Rb occupies the hcp site.

within the error bars of this analysis. In analogy to the systems K and Na adsorbed on Ru(0001),[9,10] coverage-dependent bond lengths between the Ru(0001) substrate and the alkali-metal atom have *not* been found. The driving force for flipping the adsite from fcc to hcp, when increasing the Rb coverage from $\frac{1}{4}$ to $\frac{1}{3}$, might be correlated to the onset of getting a metallic Rb overlayer; here we refer to respective discussions performed with Na-Ru(0001).[10] However, an ultimate explanation of this process of site switching has to be given by theoreticians.

[1] *Physics and Chemistry of Alkali Adsorption*, edited by H. P. Bonzel, A. M. Bradshaw, and G. Ertl (Elsevier, Amsterdam, 1989).
[2] A. Schmalz, S. Arminpirooz, L. Becker, J. Haase, J. Neugebauer, M. Scheffler, D. R. Batchelor, D. L. Adams, and E. Bøgh, Phys. Rev. Lett. **67**, 2163 (1991).
[3] J. Neugebauer and M. Scheffler, Phys. Rev. B **46**, 16 067 (1992).
[4] C. Stampfl, M. Scheffler, H. Over, J. Burchhardt, M. Nielsen, D. L. Adams, and W. Moritz, Phys. Rev. Lett. **69**, 1992 (1993).
[5] J. Neugebauer and M. Scheffler, Phys. Rev. Lett. **71**, 577 (1993).
[6] M. Nielsen, J. Burchhardt, D. L. Adams, E. Lundgren, and J. N. Andersen, Phys. Rev. Lett. **72**, 3370 (1994).
[7] J. N. Andersen, E. Lundgren, R. Nyholm, and M. Qvarford, Surf. Sci. **289**, 307 (1993).
[8] H. Over, H. Bludau, M. Skottke-Klein, G. Ertl, W. Moritz, and C. T. Campbell, Phys. Rev. B **45**, 8638 (1992).
[9] M. Gierer, H. Bludau, T. Hertel, H. Over, W. Moritz, and G. Ertl, Surf. Sci. **279**, L170 (1992).
[10] T. Hertel, H. Over, H. Bludau, M. Gierer, and G. Ertl, Surf. Sci. **301**, 1 (1994).
[11] P. M. Marcus, J. E. Demuth, and D. W. Jepsen, Surf. Sci. **53**, 501 (1975).
[12] G. Kleinle, W. Moritz, D. L. Adams, and G. Ertl, Surf. Sci. **219**, L637 (1989).
[13] J. B. Pendry, J. Phys. C **13**, 937 (1980).
[14] H. Over, W. Moritz, and G. Ertl, Phys. Rev. Lett. **70**, 315 (1993).
[15] W. Riedl and D. Menzel, Surf. Sci. **207**, 494 (1989).
[16] J. Cui, J. D. White, and R. D. Diehl, Surf. Sci. **293**, L841 (1993).
[17] J. B. Pendry, *Low Energy Electron Diffraction* (Academic, London, 1974); M. A. Van Hove, W. H. Weinberg, and C. M. Chan, *Low-Energy Electron Diffraction* (Springer, Heidelberg, 1986); M. A. Van Hove, W. Moritz, H. Over, R. J. Rous, A. Wander, A. Barbieri, N. Materer, U. Starke, and G. A. Somorjai, Surf. Sci. Rep. **19**, 191 (1993).
[18] F. Jona, K. O. Legg, H. D. Shih, D. W. Jepsen, and P. M. Marcus, Phys. Rev. Lett. **40**, 1466 (1978).
[19] H. Over, M. Gierer, and G. Ertl (unpublished).
[20] G. Kleinle, W. Moritz, and G. Ertl, Surf. Sci. **238**, 119 (1990).
[21] H. Over, U. Ketterl, W. Moritz, and G. Ertl, Phys. Rev. B **46**, 15 438 (1992).
[22] M. Gierer, H. Over, and W. Moritz (unpublished).
[23] H. Over, H. Bludau, M. Gierer, and G. Ertl (unpublished).
[24] C. Stampfl, M. Scheffler, H. Over, J. Burchhardt, M. Nielsen, D. L. Adams, and W. Moritz, Phys. Rev. B **49**, 4959 (1994).
[25] V. Fritzsche, J. B. Pendry, U. Löffler, H. Wedler, M. A. Mendez, and K. Heinz, Surf. Sci. **289**, 389 (1993).